Available online at www.sciencedirect.com
SCIENCE DIRECT®
Current Applied Physics 4 (2004) 217–220
Current Applied Physics
Physics, Chemistry and Materials Science
www.elsevier.com/locate/cap

Role of propagating ionisation fronts in semiconductor generation of sub-ps THz radiation

S.P. Jamison *, B. Ersfeld, D.A. Jaroszynski

Department of Physics, University of Strathclyde, Glasgow G4 0NG, United Kingdom

Abstract

Observations of a directional asymmetry in the sub-ps THz radiation generated from ultrafast excitation of biased GaAs are presented. This asymmetry is inconsistent with the long standing and widely accepted surface-layer current-surge description of the THz emission process. A model based on propagating carrier excitation fronts during spectral-hole-burning is proposed to explain these observations. This model introduces new roles for the semiconductor optical and carrier transport properties in determining the efficiency of the THz generation process.

PACS: 72.30.+q; 72.20.Jv; 42.65.Re; 72.20.−i; 78.20.Jq
Keywords: THz generation; Photoconductive; Spectral hole burning

1. Introduction

The established model for photoconductive THz emission from electrically biased semiconductors treats the excited conduction band region as a 2-dimensional "surface" carrier plasma, with infinitesimal thickness at the semiconductor surface [1,2]. The 2D model has been progressively improved, with increasingly realistic treatment of the carrier excitation and transport dynamics; such extensions have addressed the influence of properties such as time-dependant carrier thermalisation and mobilities [3], and ionic response to carrier currents [4]. The finite extent of the excited region has been implicitly incorporated through sub-surface diffusion dynamics, and through consideration of a non-tangential current induced by externally applied magnetic fields [5]. However, in all such investigations the THz emission itself remains treated explicitly as originating from an infinitesimally thin source.

In this paper we present experimental evidence which indicates a need to include a finite depth plasma region in the description of the THz emission process. A model is developed to account for these observations, and includes both the conduction band spectral-hole-burning propagation and the simultaneous propagation of the generated THz radiation within the carrier plasma. This description of the THz generation process predicts new roles for the semiconductor optical, far-infrared and carrier transport properties, offering the potential for enhancing the efficiency of ultrafast far-infrared sources.

2. Experimental

In the established 2D plasma model for THz generation, the boundary conditions imposed at the source require that the radiation in opposing directions, normal to the surface, have an identical time dependance [1]. Unfortunately, there are non-trivial experimental obstacles to measuring the emission in opposing directions and then directly inferring the electromagnetic fields present at the radiation source; the sub-ps time scales involved would require the far-infrared radiation paths to be independently known on a sub-100 μm scale, while the broadband, quasi single-cycle, radiation pulse emitted from the semiconductor has a temporal profile that is strongly influenced by propagation and diffraction. In the examination of the directional symmetry of THz emission presented here, such problems have been overcome by measuring the temporal profile of the emitted electric field as a function of the intensity of the ultrafast optical pulse creating the semiconductor

* Corresponding author. Tel.: +44-141-548-3103; fax: +44-141-552-2891.
E-mail address: steven.jamison@strath.ac.uk (S.P. Jamison).

1567-1739/$ - see front matter © 2003 Elsevier B.V. All rights reserved.
doi:10.1016/j.cap.2003.11.013

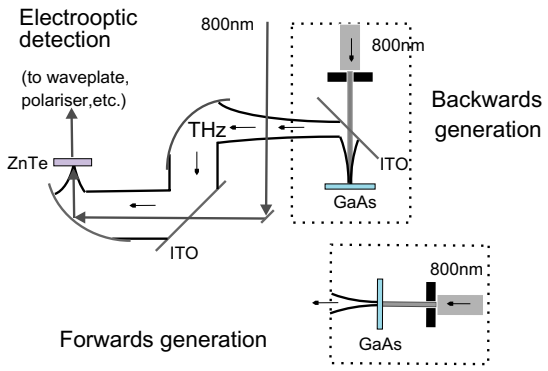

Fig. 1. Experimental layout for detecting the THz radiation generated by carriers produced in a biased slab of GaAs using a plane-wave top-hat shaped laser beam. To measure the forward and backward THz emission the emitter arrangements, shown in dashed boxes, were interchanged while maintaining the detection configuration.

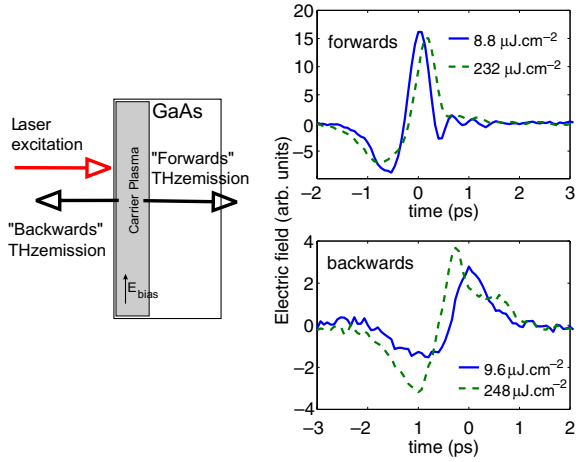

Fig. 2. THz emission detected in the forward and backward directions for differing incident power densities, showing the temporal advance and delay for backwards and forwards THz emission, respectively.

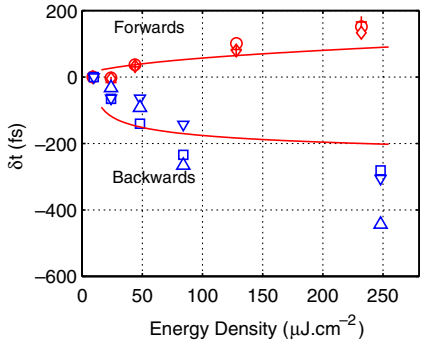

Fig. 3. Time delays for THz emission as a function of incident optical energy density. The delays of backwards emission are shown for all three definitions of THz peak (□), centroid (▽), and phase change (△). For forwards emission the time-shifts are THz peak (◊), centroid (○) and phase change (+). The solid lines are time-shifts obtained from the propagating ionisation front model discussed in the text.

plasma. While the temporal profiles of radiation detected in opposing directions cannot meaningfully be compared with significant accuracy for a given excitation intensity, the intensity dependance in opposing directions must nevertheless be identical for an infinitesimal thickness carrier plasma source.

The experimental layout is shown in Fig. 1. A 3 mJ, 800 nm, 80 fs Ti:sapphire laser system operating at repetition rate of 1 kHz provides both the carrier excitation for THz generation, and a synchronised sampling beam for electro-optic detection of the THz radiation. The emitter was a 50 mm diameter, 2 mm thick, GaAs wafer. A transverse bias field of $E_{\text{bias}} = 3\ \text{kV}\,\text{cm}^{-1}$ was applied across the semiconductor surface with electrodes separated by 3 cm. Radial variations of the excited carrier density across the GaAs slab face were minimised by using a uniform top-hat illumination profile, produced by aperturing the 1.5 cm diameter collimated visible laser beam to a 2 mm diameter spot.

Examples of the measured THz waveforms for different excitation energy densities are shown in Fig. 2. From these waveforms it can be seen that for the higher excitation energy density the peak of the THz emission is advanced in time for backward emission, while conversely it is delayed in time for the forward emission. Because the peak of the THz waveform will not necessarily provide a meaningful measurement of the time of arrival of the THz radiation, we have analysed the time shifts $\delta t \equiv t_{\text{p}} - t_{\text{ref}}$ of the THz radiation in three different ways: (1) from the peak of the THz waveform, (2) from the centroid of $|E(t)|^2$, and (3) from the change in the spectral-phase [1] $\Delta\phi = \phi(\omega) - \phi_{\text{ref}}(\omega)$ of the THz pulse. In all three cases the THz waveform obtained with the same experimental geometry and with the lowest excitation energy density was used as the reference waveform.

The energy density dependance of the time-shifts are summarised in Fig. 3. For an increasing excitation energy density an increasing time delay ($\delta t > 0$) and time advance ($\delta t < 0$) is consistently measured for the forward and backward THz emission, respectively.

The directional asymmetry in the intensity dependant THz emission time is inconsistent with an infinitesimal source thickness and, together with intensity dependant THz spectra, suggest phase-matching such as that observed in the THz emission from periodically biased ZnSe [6].

3. Propagating excitation front model

To account for the above observations of a directional asymmetry in the THz generation process a model

[1] The spectrum and phase of the THz waveforms were obtained from the fourier transform $\int E(t)\exp(\text{i}\omega t)$. A simple time shift δt of a THz pulse will therefore correspond to a phase change $\Delta\phi = \omega\delta t$.

has been developed in which the finite depth, and the associated propagation, of carrier excitation are explicitly included.

The excitation intensities used here, and as commonly used in GaAs photoconductive emitters, are sufficient to cause spectral hole burning (SHB) of the conduction band absorption. The SHB process increases the excitation skin depth to $\lesssim 10\mu m$, significantly extended beyond the linear absorption depth of ~800 nm [7]. An analytic approximation to the propagation of SHB carrier excitation front is obtained by assuming that the dominant role of the frequency dependance is in setting the saturation carrier density of the conduction band excitation, enabling the SHB to be treated as a frequency independent saturable absorption.

The coupled rate equations for the pulse energy density U, propagating with group velocity v_g, and the current density n_e are $[\partial/\partial t + v_g\partial/\partial z]U = -\alpha v_g(1-n_e/n_0)U$ and $\partial n_e/\partial t = \beta v_g(n_0 - n_e)U$. For an incident Gaussian pulse energy density $U(z=0) = U_0\exp(-t^2/\tau^2)$ this leads to an excited state carrier population

$$n_e(t,z) = n_0 - n_0[1 - F\exp(-\alpha z)]^{-1},$$

where

$$F = 1 - \exp\left(\tfrac{1}{2}\beta U_0\tau\pi^{1/2}\left[1 + \mathrm{erf}\left(\frac{t}{\tau} - \frac{z}{v_g\tau}\right)\right]\right). \qquad (1)$$

In Eq. (1), α is the linear absorption coefficient and $\beta = \alpha/n_0E_{\hbar\omega}$. Each absorbed photon of energy $E_{\hbar\omega}$ is assumed to produce a single carrier-hole pair. The saturation carrier density n_0 is estimated as 5×10^{17} cm^{-3} from the GaAs density of states within the optical excitation bandwidth of 20 nm centered at 800 nm. The carrier density evolution described by Eq. (1) is shown in the contour plots of Fig. 4 for differing excitation intensities, and includes the effects of pulse steepening during absorption of the leading edge of the optical pulse [8].

The photo-excited current, which gives rise to THz emission, is driven by an approximately static bias field E_{bias}, and is locally approximated by [2] $J(t,z) = \int_{-\infty}^{t} dt_0\rho(t_0,z)E_{bias}[1-\exp(-\nu(t-t_0))]/m^*\nu$, where ν is the carrier collisional rate, and $\rho(t_0)$ is the carrier excitation rate such that $n_e(t,z) = \int_{-\infty}^{t}\rho(t_0,z)\,dt_0$. We have simplified the model to illustrate the emission process by not including the partial cancellation of the bias field by the THz radiation field and therefore saturation of emission. The propagating radiation source term, $\partial J/\partial t$, is shown in the middle contour plots of Fig. 4.

In describing the simultaneous propagation of the THz radiation through the region of excited carriers, a Drude permittivity $\epsilon = \epsilon_{GaAs} - \omega_p^2(1+i\nu/\omega)/(\omega^2+\nu^2)$ is assumed, where $\omega_p^2 = e^2n_e(t,z)/\epsilon_0m^*$. In the calculations presented in Fig. 4 the assumed parameters for GaAs are carrier scattering rate $\nu = 10^{13}$ s^{-1}, $\epsilon_{GaAs} = 13.0$ and effective mass $m^* = 0.06\,m_e$. These GaAs properties give rise to a large THz refractive index behind the front, with typically $n \gtrsim 10$, and an absorption skin depth of $\delta \sim 2$ μm at 1 THz.

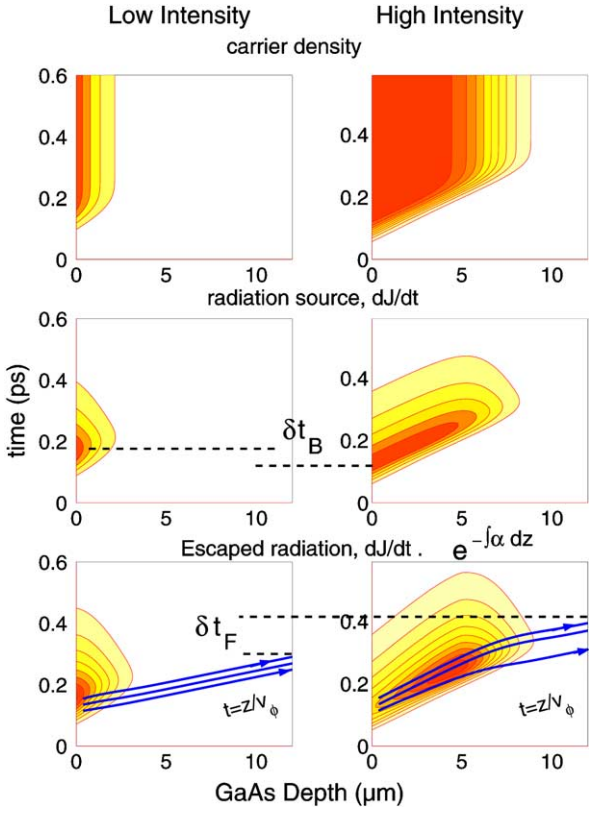

Fig. 4. Time–position contour plots of the ionisation front and THz generation. Incident 800 nm intensity (left) 16 μJ cm^{-2}, (right) 160 μJ cm^{-2}, (top) carrier density $n(t,z)$, (middle) time derivative of local current density (bottom) contours for escaped THz emission and phase front trajectories for forward emission at 1 THz.

To relate the *generated* radiation to that *emitted* from the excited carrier region, the THz phase velocity trajectories implied by the instantaneous Drude permittivity approximation have been evaluated throughout the generation region. Examples of the phase velocity trajectories for forward emission, at a frequency of 1 THz, are shown in the lower plots of Fig. 4. The 'emitted' radiation shown in the contour plots of Fig. 4, also for a frequency of 1 THz, is obtained by weighting the generated radiation with the integrated absorption along these phase trajectory paths: $\partial J(z,t)/\partial t \times \exp\{-\int_{z,t}^{z\to\infty}\alpha_{THz}(z')\,dz'\}$, where the integration is along the phase velocity path, and $\alpha_{THz} = \Im m\{\epsilon^{1/2}\}\omega/c$ is the THz absorption coefficient.

4. Discussion

Backward emission: The absorption of THz frequencies in the presence of carriers ensures that only the region within the THz skin depth of the surface

contributes to backward emission. The dominant factor in the emission time is therefore the time of carrier excitation within a region close to the semiconductor surface. For increasing excitation energy density the carrier excitation will advance in time as the saturation carrier density is obtained from progressively earlier parts of the optical pulse leading edge. The predicted time advance δt_B with increasing excitation energy density, as estimated by the time of the maximum $\partial J/\partial t$ at the semiconductor surface, is indicated in the $\partial J/\partial t$ contours of Fig. 4. For comparison with the experimental data this time advance estimate is also shown as a solid line in Fig. 3.

Forward emission: For forward emission the relative propagation velocities of the carrier excitation front and the THz radiation will be a dominant factor in the observed THz emission. In GaAs the carrier excitation front propagates slower than the group velocity of 800 nm radiation ($v_g = c/4.2$), due to the erosion of the pulse front by SHB [8], and consequently also slower than the THz phase velocity in unexcited GaAs ($v_\phi \sim c/3.6$ at THz frequencies). Conversely, due to the carrier density dependant permittivity behind the excitation front, THz radiation generated behind the front travels even slower and will remain trapped behind the front. High absorption in the plasma region will rapidly erode this trapped radiation. Radiation generated within a skin depth of the collapsing edge of front, at the maximum SHB depth, dominates the emitted radiation. The trapping of radiation behind the front is apparent in the phase velocity trajectories of Fig. 4, while the strong self absorption of the carrier plasma can be seen in the peak emission contours occurring at a depth of $\sim$5 μm in the high intensity calculation. The time delay δt_F of the forward emission indicated by the phase velocity trajectories of Fig. 4. An approximate time delay is estimated from the time delay associated with the collapse of the excitation front compared to the THz propagation time in unexcited GaAs, and is shown in comparison with the experimental data in Fig. 3.

In summary, we have observed a directional asymmetry in the excitation intensity dependance of THz emission from a GaAs photoconductive emitter that is inconsistent with the established description of such THz sources. A new model has been proposed in which the combined effect of spectral hole burning and the permittivity of the carrier plasma behind the SHB front is responsible for this directional asymmetry. This model invokes significantly new roles for the material properties in determining the efficiency of the THz generation process; it explicitly introduces the relative propagation of both the optical and generated far-infrared radiation, and the self absorption of far-infrared radiation in the excited semiconductor. It is speculated that recognition of the role of propagating carrier excitation in standard semiconductor THz emitters may lead to identification of superior materials and excitation conditions for efficient ultrafast THz generation. Application of external magnetic fields to reduce the THz absorption also has the potential for enhancement of photoconductive THz emitters.

Acknowledgements

The technical assistance of D. Clark and financial support from the Scottish Higher Education Funding Council and the Engineering and Physical Sciences Research Council are gratefully acknowledged.

References

[1] J.T. Darrow, X.-C. Zhang, D.H. Auston, IEEE J. Quant. Elec. 28 (1992) 1607.
[2] C.W. Siders, J.L.W. Siders, A.J. Taylor, G.-G. Park, M.R. Melloch, A.M. Weiner, Opt. Lett. 24 (1999) 241;
P.U. Jepsen, R.H. Jacobsen, S.R. Kieding, J. Opt. Soc. Am. B 13 (1996) 2424.
[3] A.J. Taylor, P.K. Benicewicz, S.M. Young, Opt. Lett. 18 (1993) 1340.
[4] A. Leitenstorfer, S. Hunsche, J. Shah, M.C. Nuss, W.H. Knox, Phys. Rev. Lett. 82 (1999) 5140.
[5] M.B. Johnston, D.M. Whittaker, A. Corchia, A.G. Davies, E.H. Linfield, Phys. Rev. B 65 (2002) 165301.
[6] D. Hashimshony, A. Zigler, K. Papadopoulos, Phys. Rev. Lett. 86 (2001) 2806.
[7] J.L. Oudar, D. Hulin, A. Migus, A. Antonetti, F. Alexandre, Phys. Rev. Lett. 55 (1985) 2074;
S. Hunsche, H. Hessel, A. Ewertz, H. Kurz, J.H. Collet, Phys. Rev. B 48 (1993) 17818.
[8] M. Adachi, Y. Masumoto, Phys. Rev. Lett. 40 (1989) 2908.